Available online at www.sciencedirect.com
SCIENCE DIRECT®
Journal of Sound and Vibration 280 (2005) 455–465
JOURNAL OF SOUND AND VIBRATION
www.elsevier.com/locate/jsvi

Short Communication

Multi-stage regression fatigue analysis of non-Gaussian stress processes

Xiangyu Wang, J.Q. Sun*

Department of Mechanical Engineering, University of Delaware, Newark, DE 19716, USA

Received 5 January 2004; accepted 5 February 2004
Available online 17 September 2004

1. Introduction

Structural fatigue can be predicted either in the time domain or frequency domain. In the time domain, a large number of stress responses are simulated. Cycle counting methods are used to identify damage events. It is generally accepted that the rainflow cycle counting method is the best method to identify damage events of a broad-band random stress response. From the so-called rainflow cycles, fatigue life can be obtained using Palmgren and Miner's linear accumulative damage rule. The time domain method is suitable for simple structures where only a few hot spots need to be investigated. For large structures, computations become intensive. Fatigue analysis of such structures generally uses frequency domain methods. In the frequency domain, fatigue life is calculated from the power spectral density (PSD) of the stress response. Neither time history samples of the stress processes nor a cycle counting procedure will be needed. The frequency domain methods are much less computationally intensive than the time domain methods. This paper proposes a frequency domain procedure to calculate the fatigue life of structures with stationary non-Gaussian stress processes.

Stress processes can be classified as Gaussian or non-Gaussian in terms of their probability density functions (PDF), narrowband or broadband in terms of their PSDs. Different frequency domain methods have been proposed to predict fatigue life where the stress process has a different

*Corresponding author. Tel.: 302-831-8686; fax: 302-831-3619.
E-mail address: sun@me.udel.edu (J.Q. Sun).

0022-460X/$ - see front matter
doi:10.1016/j.jsv.2004.02.036

combination of PDFs and PSDs. The simplest case is when the stress is Gaussian and narrowband. When the stress process is non-Gaussian and broadband, the fatigue analysis becomes much more difficult. Dirlik [1] proposed an empirical closed-form expression for the PDF of rainflow ranges from extensive Monte Carlo simulations. Bishop and Sherratt [2] were able to obtain a theoretical solution to the PDF of rainflow ranges using the Markov chain theory after adopting a new definition of the rainflow range. Wirsching and Light [3] obtained the correction factor for the fatigue prediction of narrow-band Gaussian processes as a function of the spectral width parameter and the exponential coefficient of the S–N curve [3]. Lutes et al. [4] suggested an adjustable bandwidth factor. Ortiz and Chen [5] adopted a new definition for the adjustable bandwidth measure and proposed an empirical expression to calculate the optimum order of moments involved. Tovo [6] showed that the rainflow damage is bounded and proposed that it can be calculated as a linear combination of the two bounds. The formula obtained by curve-fitting numerical simulation results gives accurate approximations of fatigue damage under both broad- and narrow-band Gaussian loading. Winterstein [7] investigated the effect of the non-Gaussianity in terms of kurtosis on the mean damage rate. Winterstein [8] further developed a more accurate second order expression using an approximate Weibull distribution to fit the stress range. Lutes and Wang [9] compared the accuracy of these approximations of the non-Gaussian effect. Sarkani et al. [10] also found out that the non-normality can significantly influence the rate of fatigue damage accumulation, from their analytical studies, as well as fatigue experiments on welded cruciform specimens.

When the stress process is broadband and non-Gaussian, the fatigue analysis becomes very complicated. Few formulas are available in the literature. Lutes et al. [4] suggested the use of two correction factors for the Gaussian and narrowband assumption: a bandwidth correction factor and a non-normality correction factor. The main contribution of the present paper is the development of a methodology for fatigue prediction of structures with broad-band and non-Gaussian stress response.

The remainder of the paper is organized as follows. In Section 2 we review the method we used to simulate non-Gaussian time histories with a prescribed PSD function, and the adaptive kernel method to estimate the distribution of rainflow ranges. In Section 3 a multi-stage regression method is developed to obtain the PDF function for the rainflow stress ranges in terms of the bandwidth and non-normality parameters of the stress process. We then validate the proposed PDF model using new simulation data which are not used in the regression analysis. In Section 4 we show that the fatigue prediction using the proposed PDF model agrees well with simulations. In Section 5 we conclude the paper with some remarks.

2. Preliminaries

2.1. Simulation of non-Gaussian processes

2.1.1. Probability distribution

A common technique for simulating a second-order non-Gaussian process $X(t)$ is by means of a transformation $g(\cdot)$ of a standard Gaussian process $U(t)$ with unit variance and zero mean,

defined as [11]

$$X(t) = g(U(t)) = F_X^{-1}[\Phi[U(t)]], \tag{1}$$

where $\Phi[\cdot]$ and $F_X[\cdot]$ are the cumulative distribution functions of the standard Gaussian and non-Gaussian processes, respectively. The stress distribution of virtually any nonlinear structural response can be matched by applying an appropriate monotonic transformation $g(\cdot)$. Moreover, $g(\cdot)$ can be approximated by a Hermite polynomial expansion [8],

$$X_0 \equiv \frac{X - \mu_X}{\sigma_X} = k\left[U + \sum_{n=3}^{N} a_n H_{n-1}(U)\right], \tag{2}$$

where μ_X and σ_X are the mean and standard deviation of $X(t)$, respectively. k is a scaling factor ensuring that $X_0(t)$ has unit variance. $H_n(u)$ is the nth-order Hermite polynomial, $H_n(u) = (-1)^n \exp(u^2/2)\,(\mathrm{d}^n/\mathrm{d}u^n)\exp(-u^2/2)$. From here on, we will work with the normalized stress process $X_0(t)$ since the original process $X(t)$ can be obtained from $X(t) = \sigma_X X_0(t) + \mu_X$.

As an example, we truncate Eq. (2) at $N = 4$,

$$X_0(t) = k[U + a_3(U^2 - 1) + a_4(U^3 - 3U)]. \tag{3}$$

The coefficients can be determined by matching the moments of $X_0(t)$ up to fourth order for a symmetric distribution as

$$k = \frac{1}{\sqrt{1 + 6a_4^2}}, \quad a_3 = 0,$$
$$\alpha_4 = \frac{1}{(1 + 6a_4^2)^2}(3348a_4^4 + 1296a_4^3 + 252a_4^2 + 24a_4 + 3). \tag{4}$$

2.1.2. Spectral distribution

The spectral properties of the process $X_0(t)$ can be captured by imposing an appropriate correlation structure on the process $U(t)$. The correlation of $X_0(t)$ is related to that of $U(t)$ by the following expression for $N = 4$:

$$R_{X_0X_0}(t) = k^2[R_{UU}(t) + 2a_3^2 R_{UU}(t)^2 + 6a_4^2 R_{UU}(t)^3], \tag{5}$$

where $R_{X_0X_0}(t)$ and $R_{UU}(t)$ are the correlation functions of $X_0(t)$ and $U(t)$. In this paper, we would like to sample the PDF and PSD functions of the process $X_0(t)$ in a broad range and in a random manner in order to develop a regression model that has an ability to generalize. For this reason, we pick the corresponding correlation function $R_{UU}(t)$ for the Gaussian process $U(t)$. Eq. (5) is then used to calculate the correlation function $R_{X_0X_0}(t)$.

In the numerical examples presented later, we consider the following spectral density function of $U(t)$:

$$\Phi_{UU}(\omega) = \frac{\Phi_1}{(\omega_1^2 - \omega^2)^2 + (2\varsigma_1\omega_1\omega)^2} + \frac{\Phi_2}{(\omega_2^2 - \omega^2)^2 + (2\varsigma_2\omega_2\omega)^2}. \tag{6}$$

In the numerical examples, seven values of kurtosis of $X_0(t)$ are studied: $\alpha_4 = 4$, 7, 10, 14, 17, 20, and 24. For each kurtosis, various PSD functions of $U(t)$ are chosen in such a way that the irregularity factor of the corresponding non-Gaussian stress process $X_0(t)$ assumes values ranging from 0 to 1 with an increment of about 0.05. For each combination of kurtosis and irregularity factor, 10 stress samples are simulated and each sample has 2^{15} points. The simulated stress samples are then put through the rainflow counting procedure to collect the rainflow ranges. For each combination of kurtosis and irregularity factor, the number of rainflow range samples collected is generally more than 100,000.

2.2. Density estimation

The histogram of the rainflow ranges of a non-Gaussian stress process shows a long tail which has a significant influence on the fatigue life prediction because the fatigue analysis involves higher order moments of the rainflow ranges. It is therefore important to estimate the tail part of the probability density function as accurately as possible. An adaptive kernel method is adopted in this paper [12].

The adaptive kernel estimate $\widehat{f}(s)$ of a probability density function $f(s)$ can be expressed as

$$\widehat{f}(s) = \frac{1}{n}\sum_{i=1}^{n} \frac{1}{\lambda_i h} K\left(\frac{s - S_i}{\lambda_i h}\right), \tag{7}$$

where $\lambda_i = [\widetilde{f}(S_i)/\bar{f}]^{-\theta}$ is a local window width factor, θ is the sensitivity parameter such that $0 \leqslant \theta \leqslant 1$, n is the total number of the sample data, h is the window width, S_i are the sample data

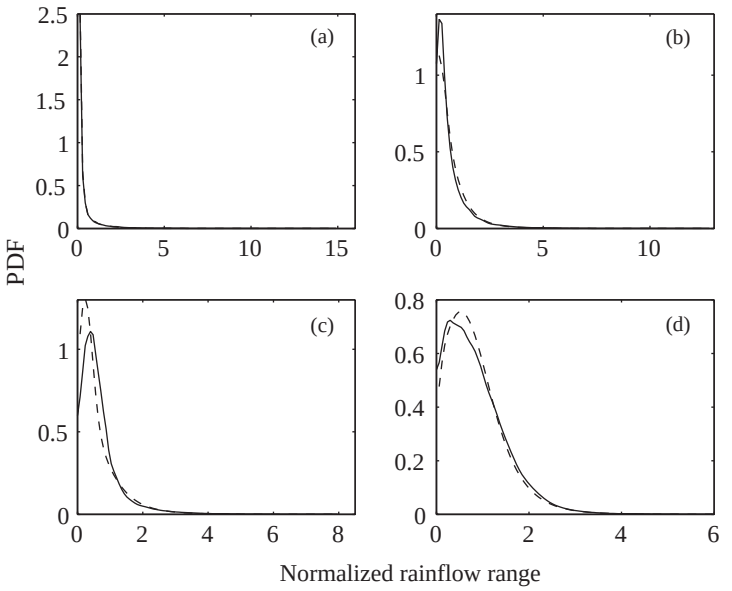

Fig. 1. PDF of the rainflow range. Solid line: estimates from the adaptive kernel method. Dashed line: the predictions from Eq. (9). (a) $\alpha_4 = 20$, $r = 0.355$, $m = 0.215$. (b) $\alpha_4 = 14$, $r = 0.770$, $m = 0.663$. (c) $\alpha_4 = 7$, $r = 0.659$, $m = 0.49$. (d) $\alpha_4 = 4$, $r = 0.905$, $m = 0.863$.

points and $K(\cdot)$ is a kernel function. $\widetilde{f}(s)$ is a pilot estimate of $f(s)$ and $\overline{f}$ is a geometric mean of $\widetilde{f}(s)$. In this paper, we set $\theta = 1/2$. The conventional kernel estimate when $\lambda_i = 1$ is used to calculate $\widetilde{f}(s)$. The kernel is chosen to be Gaussian.

Some typical plots of the estimate of the distribution of the rainflow ranges are shown in Fig. 1. It can be seen that the adaptive kernel method not only captures the mode in the rainflow range distribution but also gives a good approximation of the long tail.

3. Multi-stage regression of rainflow stress ranges

3.1. Choice of independent variables

Among many factors of the stress process affecting the fatigue, in this work, we consider the following four: the standard deviation σ_X of the stress process, the mean frequency, the irregularity factor of the PSD, and the kurtosis, α_4, of the probability density. We further assume that the PDF of the stress process is a symmetrical non-Gaussian distribution.

Let η_i denote the ith-order spectral density moment defined as

$$\eta_i = 2\int_0^\infty \omega^i \Phi_{X_0X_0}(\omega)\,\mathrm{d}\omega, \tag{8}$$

where $\Phi_{X_0X_0}(\omega)$ is the PSD of the stress process $X_0(t)$. Note that $\eta_0 = \sigma_X^2$. A common definition of the irregularity factor $r = \eta_2/\sqrt{\eta_0\eta_4}$ is adopted as the bandwidth parameter. A dimensionless frequency $m = (\eta_1/\eta_0)\sqrt{\eta_2/\eta_4}$ is taken as the mean frequency [1].

It is common to use a normalized rainflow range $z = s/(2\sigma_X)$ in the PDF estimation where s is a rainflow stress range. The effect of σ_X is then automatically included and will not be considered explicitly. In the end, we shall work with three independent variables: the kurtosis of the probability density α_4, the mean frequency m, and the irregularity factor r of the PSD. Finally, we point out that the choice of α_4, m and r as independent variables is totally empirical as is done in Ref. [2]. Nevertheless, the methodology developed in this paper will be valid for other choices of independent variables.

3.2. Regression model of the rainflow range PDF

After carefully studying the estimated PDFs of the rainflow range of the simulated stress processes, we propose the following function form for the PDF of the rainflow range:

$$f(z) = c_1\frac{1}{\tau}\,\mathrm{e}^{-z/\tau} + c_2\frac{z}{\alpha^2}\,\mathrm{e}^{-(z/\alpha)^{2/2}} + c_3\frac{1}{\sqrt{2\pi}\beta z}\,\mathrm{e}^{-(\ln z/\beta)^{2/2}}, \tag{9}$$

where $c_1, c_2, c_3, \tau, \alpha$ and β are coefficients to be determined using the least squares method. $f(z)$ contains three common density functions: exponential, Rayleigh and lognormal, which together can model a broad range of PDFs. The normalization of the density function leads to

$$c_1 + c_2 + c_3 = 1. \tag{10}$$

Fatigue calculation involves higher-order moments of rainflow ranges. The order of the moment is related to the slope b of the logarithmic S–N curve. Assume that the slope b is an

integer for now. We impose the following moment constraint for $f(z)$:

$$\int f(z)z^b \,\mathrm{d}z = c_1\tau^b\Gamma(1+b) + c_2\left(\sqrt{2}\alpha\right)^b\Gamma\left(1+\frac{b}{2}\right) + c_3\,\mathrm{e}^{(1/2)(b\beta)^2} = m_b, \tag{11}$$

where m_b is the bth-order moment of the stress range determined from the rainflow counting. For common engineering materials, the slope b varies between 2 and 6 [13]. In the examples, we choose $b = 6$. If b is a decimal, we impose the moment constraint of an integer order which is the round-up of b.

The coefficients in $f(z)$ are functions of various characteristic parameters of the stress process including the kurtosis α_4, the mean frequency m, and the irregularity factor r. Our goal is to relate the coefficients in $f(z)$ to these characteristic variables of the stress process. Note that Eq. (10) reduces the number of independent coefficients to five while Eq. (11) does not.

3.3. Multi-stage regression

When the coefficients $c_1, c_2, c_3, \tau, \alpha$ and β of $f(z)$ are assumed functions of the kurtosis, irregularity factor and mean frequency of the stress process, the regression analysis to determine $f(z)$ and its coefficients becomes a multidimensional curve-fitting problem. This requires a large set of data due to the curse of dimensionality in statistics. Moreover, it is difficult to choose a function form for the coefficients, which is a critical step in regression analysis. With a limited but reasonable set of data, we propose a multi-stage regression approach to create a functional relationship between $f(z)$ and its coefficients and the chosen independent variables of the stress process.

3.3.1. The first stage

In the first stage, we apply the least squares method to determine $f(z)$ for all the stress samples with different independent variables, subject to constraint (11). This process leads to a collection of the coefficients $c_1, c_2, c_3, \tau, \alpha$ and β.

3.3.2. The second stage

Recall that only five of the six coefficients are independent. We need to choose five coefficients and develop functional relationships with the independent stress variables. We have chosen c_1, c_3, τ, α and β.

Hereafter, we use β as an example to demonstrate the multi-stage regression method. Fig. 2 shows the collection of the coefficient β from the first stage regression. β is plotted against a compound parameter m/r. A linear relationship emerges,

$$\beta = \varepsilon_1\frac{m}{r} + \varepsilon_2, \tag{12}$$

where ε_i $(i = 1, 2)$ are unknown parameters, which assume different values for stress processes with varying kurtosis values. In the subsequent stage, we will fit ε_i as a function of the kurtosis α_4. The compound parameter m/r has been identified with extensive numerical experimentations, and helps to reduce an otherwise two-dimensional regression problem with respect to m and r to a one-dimensional regression. This alleviates the need for a large number of data.

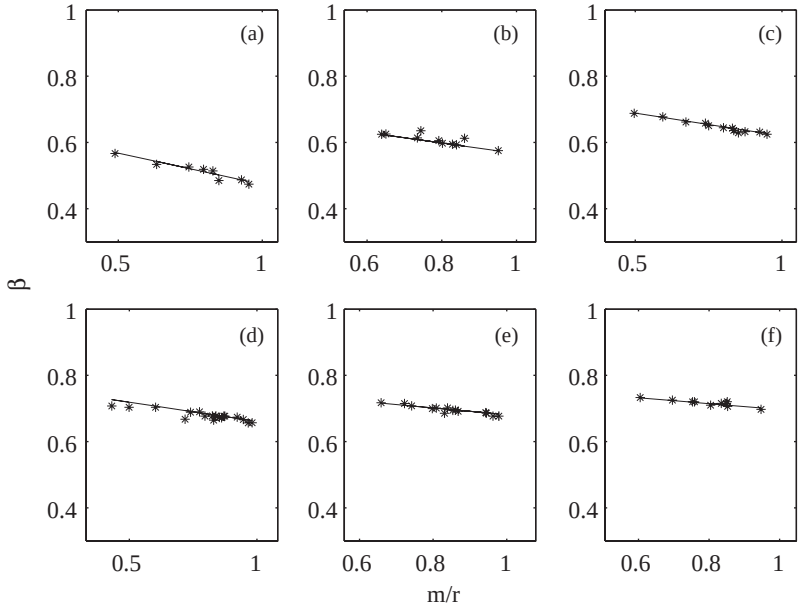

Fig. 2. Examples of β as a function of m/r for different stress processes. *: represents results from the regression analysis of the rainflow range distribution. Solid line: prediction from Eq. (14). The kurtosis is (a) $\alpha_4 = 4$, (b) $\alpha_4 = 7$, (c) $\alpha_4 = 10$, (d) $\alpha_4 = 14$, (e) $\alpha_4 = 17$, (f) $\alpha_4 = 20$.

3.3.3. The third stage

In this stage of regression, we express ε_i as a function of the kurtosis α_4. From the data, we observe that ε_1 increases with the kurtosis almost linearly with a slowly varying slope and that ε_2 grows exponentially with the kurtosis [14]. The following regression results are obtained:

$$\varepsilon_1 = 0.10551\alpha_4^{0.3} - 0.34815, \quad \varepsilon_2 = 0.78883 - 0.32239e^{-0.23263\alpha_4}. \tag{13}$$

Fig. 3 shows the results of the regression of ε_i as a function of α_4.

The final expression for the coefficient β becomes

$$\beta = (0.10551\alpha_4^{0.3} - 0.34815)\frac{m}{r} + 0.78883 - 0.32239e^{-0.23263\alpha_4}. \tag{14}$$

Fig. 2 shows the predictions of β from Eq. (14). The agreement of the predictions with the simulated data in a broad range of the variables α_4, r and m is excellent.

3.3.4. An iterative procedure

When the regression results for c_1, c_3, τ, α and β are substituted into Eq. (9), the error from the regression will inevitably propagate to the PDF model of the rainflow range. One way to enhance the accuracy of the prediction of Eq. (9) is to introduce an iterative procedure to improve the fitting of the PDF coefficients.

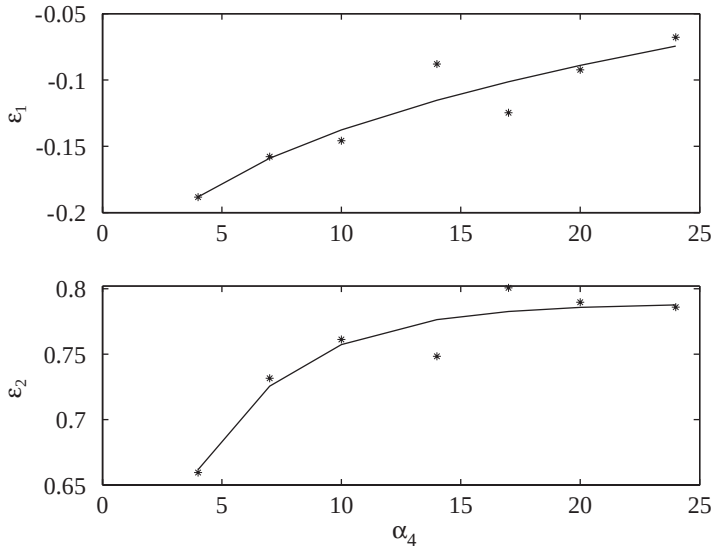

Fig. 3. The regression results of $\varepsilon_i, i = 1, 2$ with respect to α_4 in the third stage regression. ∗: represents results from the second stage regression. Solid line: the prediction from Eq. (13).

In the iterative procedure, the regression function of a coefficient is substituted into Eq. (9) as soon as it is obtained. The least squares analysis of the updated Eq. (9) is conducted to obtain the remaining coefficients.

For example, we can substitute the value of β from Eq. (14) in Eq. (9). α can be determined by the multi-stage regression method as in Eq. (15). Then the regression results of β and α are substituted in Eq. (9) together to determine the remaining coefficients c_1, c_3 and τ. Following this procedure, we obtain

$$\begin{aligned}
\alpha &= 0.00142\alpha_4^2 - 0.051\alpha_4 + 0.2175 \\
&\quad - (0.03342\alpha_4^2 - 1.159\alpha_4 - 1.5925)\left[\frac{m(m^{0.1}-1)}{r(r^{0.7}-1)}\right]^2, \\
\tau &= (-1.8313\alpha_4 + 68.9345)\left(\frac{1.6r-m}{r^{0.1}+1}\right)^2 \\
&\quad + (0.872\alpha_4 - 30.0846)\left(\frac{1.6r-m}{r^{0.1}+1}\right) - 0.1\alpha_4 + 3.3822, \\
c_1 &= \max(0,\ \tau[(0.04406\alpha_4^2 - 1.229\alpha_4 - 6.654)(1.6r-m) \\
&\quad - 0.02688\alpha_4^2 + 0.8025\alpha_4 + 3.953]), \\
c_3 &= \max\left[0,\ (0.1494\alpha_4^2 - 3.6391\alpha_4 + 28.0776)\left(\frac{r}{r+2m}\right)^2\right.
\end{aligned}$$

$$- (0.1323\alpha_4^2 - 3.2923\alpha_4 + 27.9722)\left(\frac{r}{r+2m}\right) + 0.0293\alpha_4^2 - 0.7475\alpha_4 + 7.0789\Bigg],$$

$$c_2 = \max(0,\, 1 - c_1 - c_3), \tag{15}$$

where $\max(\cdot,\cdot)$ returns the maximum of its arguments.

This iterative process can continue by retaining the functions of some of the coefficients in $f(z)$ and obtaining the functions for the remaining coefficients by the multi-stage regression method. In a related study, we have found that the procedure usually converges in a small number of iterations [15]. Nevertheless, a rigorous proof of convergence of the iterative procedure is elusive at this time.

3.4. Validation of the regression model

Fig. 1 shows that the prediction from Eq. (9) generally agrees well with the density estimate from the adaptive kernel method. The prediction is not satisfactory near the origin in some cases, but is quite accurate in the middle to tail portion of the distribution. This is important for the fatigue analysis.

In order to validate the multi-stage regression model beyond the set of data on which the model is developed, a new stress process is generated. The parameters of the process are: $\sigma_X = 20$, $\alpha_4 = 12$, $r = 0.536$ and $m = 0.426$. The rainflow range distribution from the simulated data and the prediction from Eq. (9) agree as well as in Fig. 1. This validates the proposed regression model of the probability density of rainflow ranges.

4. Fatigue prediction

One of the important applications of Eq. (9) is to facilitate the calculation of fatigue life. With the help of Eq. (9), we are able to predict the fatigue life directly from the stress response, thus bypassing the time-consuming rainflow counting over a large set of time histories.

In the study of fatigue, we adopt the S–N model as [13]

$$N_F S^b = K_s, \tag{16}$$

where N_F is the number of cycles to failure under a sinusoidal stress with constant amplitude. S is the stress range. b and K_s are material constants. For high cycle fatigue, the Palmgren–Miner accumulative damage theory can be applied [13]. The average damage per cycle is

$$\overline{\Delta D} = \frac{1}{K_s}\int_0^\infty s^b \rho(s)\,\mathrm{d}s, \tag{17}$$

where $\rho(s)$ is the PDF $f(s/(2\sigma_X))$ of the rainflow range in Eq. (9) obtained by the multi-stage regression. We assume that the mean of the stress cycle is zero. However, one can modify the S–N equation to account for the effect of mean stress on fatigue life [16].

Table 1
Comparison of fatigue predictions by Monte Carlo simulations and Eq. (18)

Stress process	Fatigue prediction		
	Simulation	Eq. (18)	90% Confidence interval
(a)	3.937×10^6	3.972×10^6	$[3.659 \times 10^6, 4.198 \times 10^6]$
(b)	6.678×10^6	5.565×10^6	$[6.333 \times 10^6, 6.958 \times 10^6]$
(c)	3.487×10^7	3.276×10^7	$[3.273 \times 10^7, 3.680 \times 10^7]$
(d)	1.843×10^8	1.776×10^8	$[1.768 \times 10^8, 1.905 \times 10^8]$

The stress processes (a)–(d) refer to Fig. 1.

Fatigue failure is said to occur when the accumulated damage reaches unity. Assume that the average damage per cycle is constant. The mean fatigue life in cycles is given by

$$N_m = \frac{1}{\overline{\Delta D}} = \frac{K_s}{(2\sigma_X)^b m_b}. \tag{18}$$

Note that m_b can be calculated from Eq. (11).

In the numerical examples, we have used the material constants $b = 6$, and $K_s = 3.096 \times 10^{19}$. To establish a baseline for checking the accuracy of the fatigue life prediction based on the regression model, we use Monte Carlo simulations to obtain the fatigue life estimate from the raw time histories of the stress. We first simulate a large number of time histories of the stress process. The rainflow cycle counting scheme is applied to calculate the fatigue life. The bootstrap method [17] is used to calculate the 90% confidence interval of the fatigue life prediction.

The stress processes with the rainflow range distribution shown in Fig. 1 are used as examples. The standard deviation of all of the stress processes is assumed to be 20. The fatigue life from the Monte Carlo simulation and from Eq. (18) based on the regression model are listed in Table 1. It can be seen that the prediction from Eq. (18) falls in the 90% confidence interval or slightly outside the interval but on the conservative side, and therefore agrees well with the result of Monte Carlo simulation statistically.

Another example is presented here to show the prediction ability of Eq. (18) by using the new stress process with the parameters $\sigma_X = 20$, $\alpha_4 = 12$, $r = 0.536$ and $m = 0.426$. The mean fatigue life from the Monte Carlo simulations is 8.436×10^6 cycles with a 90% confidence interval: $[7.792 \times 10^6, 8.916 \times 10^6]$. The fatigue life predicted from Eq. (18) based on the regression model is 7.744×10^6. It is very close to the lower bound of the 90% confidence interval. Thus, Eq. (18) provides conservative and reasonably accurate fatigue life estimates.

5. Concluding remarks

A multi-stage regression method has been proposed to obtain an empirical PDF model for the rainflow ranges of non-Gaussian stress processes. The proposed PDF model captures the non-Gaussian properties of a wide range of stress processes characterized by four parameters: standard

deviation, kurtosis, irregularity factor and mean frequency. A higher order moment constraint is proposed to improve the accuracy of the regression model of the rainflow stress range PDF. The regression model has been validated with simulated stress processes that have not been used in the regression analysis. The resulting closed-form empirical PDF of rainflow ranges enables us to carry out fatigue analysis efficiently and accurately. The fatigue life predictions based on the regression model agree very well with those from extensive Monte Carlo simulations.

References

[1] T. Dirlik, Application of Computers in Fatigue Analysis, PhD Dissertation, University of Warwick, 1985.
[2] N.W.M. Bishop, F. Sherratt, A theoretical solution for the estimation of rainflow ranges from power spectral density data, *Fatigue and Fracture of Engineering Materials and Structures* 13 (4) (1990) 311–326.
[3] P.H. Wirsching, M.C. Light, Fatigue under wide band random stresses, *Journal of the Structural Division, Proceedings of the American Society of Civil Engineering* 106 (ST7) (1980) 1593–1607.
[4] L.D. Lutes, M. Corazao, S.l.J. Hu, J. Zimmerman, Stochastic fatigue damage accumulation, *Journal of Structural Engineering* 110 (11) (1984) 2585–2601.
[5] K. Ortiz, N.K. Chen, Fatigue damage prediction for stationary wideband random stresses, in: *Proceedings of the Fifth International Conference on Applications of Statistics and Probability in Soil and Structural Engineering*, (ICASP 5), Vancouver, British Columbia, Canada, 1987, pp. 309–316.
[6] R. Tovo, Cycle distribution and fatigue damage under broad-band random loading, *International Journal of Fatigue* 24 (2002) 1137–1147.
[7] S.R. Winterstein, Non-normal responses and fatigue damage, *Journal of Engineering Mechanics* 111 (10) (1985) 1291–1295.
[8] S.R. Winterstein, Nonlinear vibration models for extremes and fatigue, *Journal of Engineering Mechanics* 114 (10) (1988) 1772–1790.
[9] L.D. Lutes, J. Wang, Kurtosis effects on stochastic structural fatigue, in: *Proceedings of the International Conference on Structural Safety and Reliability*, Innsbruck, Austria, 1993, pp. 1091–1097.
[10] S. Sarkani, D.P. Kihl, J.E. Beach, Fatigue of welded joints under narrowband non-Gaussian loadings, *Probabilistic Engineering Mechanics* 9 (3) (1994) 179–190.
[11] M. Grigoriu, Simulation of stationary non-Gaussian translation processes, *Journal of Engineering Mechanics* 124 (2) (1998) 121–126.
[12] B.W. Silverman, *Density Estimation for Statistics and Data Analysis*, Chapman & Hall, New York, 1986.
[13] N.E. Dowling, *Mechanical Behavior of Materials*, Prentice-Hall, Englewood Cliffs, NJ, 1993.
[14] G.E.P. Box, D.R. Cox, An analysis of transformations, *Journal of the Royal Statistical Society* (1964) 211–243.
[15] X. Wang, J. Eisenbrey, M. Zeitz, J.Q. Sun, Multi-stage regression analysis of acoustical properties of polyurethane foams, *Journal of Sound and Vibration* 273 (2004) 1109–1117.
[16] X. Wang, J.Q. Sun, Structural fatigue life prediction with system uncertainties, *Journal of Sound and Vibration* 257 (5) (2002) 977–984.
[17] M.R. Chernick, *Bootstrap Methods: A Practitioner's Guide*, Wiley, New York, 1999.